A Space-Based Microwave Radar Concept

D. Chakraborty, *Senior Member, IEEE*

***Abstract*—A Space-Based Microwave Radar (SBR) Concept is defined using a tether trans/receive antenna supported between two gravity gradient low earth-orbiting satellites. A cluster of four tether antennas each of 6 km maximum length and 1.5 km separation between tethers constitutes a radar. A system of 8 to 11 such clusters constitutes the overall radar scheme which will cover approximately one third of the earth surface for detecting sea-based targets. Issues identified are the array structure, coherence of tethered arrays, grating lobe energy clamping, clutter effects, communications, system requirements and the overall radar system concept including stability considerations. This paper presents the base-line definition of an alternate space-based radar scheme. A significant amount of R&D efforts will be required to derive practical solutions of the proposed scheme.**

I. Introduction

If a long array of vertical dipoles could be suspended between two low orbiting satellites (altitude $\simeq 900$ km) separated by several kilometers and if the perturbations of these satellite movements could be controlled within a reasonable tolerance then a light weight very long radiating/receiving aperture could be created. By feeding each element with a fraction of a watt transmit power a large power-aperture (watt-m^2) parameter can be generated. Reciprocally, using cost effective Schottky diode mixers or GaAs low-noise converters or LNA's on chips via diode type T/R switches, each element of the array could act as a distributed receiving element. By computer control the phase of each of the transmitting elements or a group of elements could be varied to produce beam scanning. Superposition of the received signals from each element will provide the desired signal-to-noise ratio at the detector. This scheme was conceived by the late Dr. Harry Davis in an unpublished report.

The system geometry is outlined in Fig. 1 and the system architecture is shown in Fig. 2 where satellite #1 in a cluster of four satellites is acting as the cluster controller. Satellites #2, 3, and 4 are linked by radio with the cluster controller. A fiber optic common addressing bus (LAN-Local Area Network) for beam scanning and T/R waveform transmission is assumed. Transmit pulses are addressed to different subarrays in a tether. Four tethers are squentially excited to generate ($m \times n$) cell scanning

Manuscript received May 5, 1991; revised December 12, 1991.
The author is with the Jet Propulsion Laboratory, California Institute of Technology, 4800 Oak Grove Drive, Pasadena, CA 91109.
IEEE Log Number 9107458.

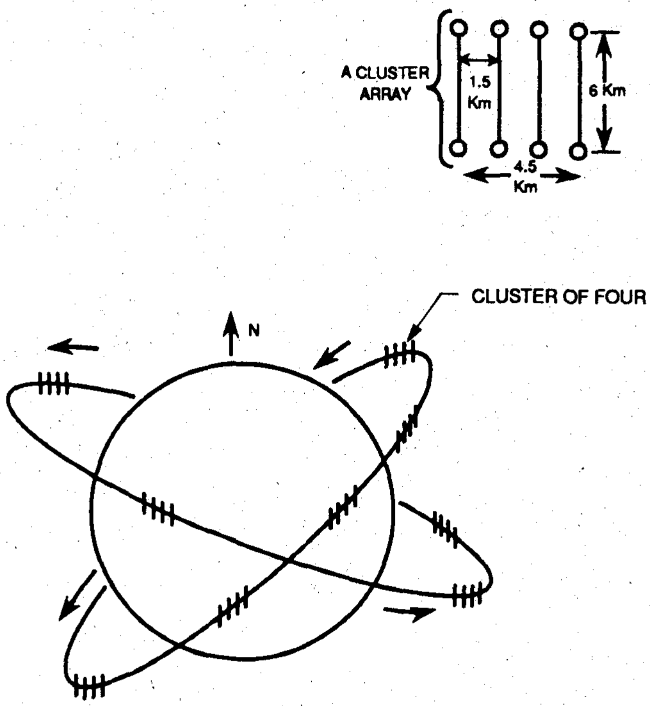

Fig. 1. Space based radar geometry.

where m is the number of parallel tethers and n is the number of elements in each tether.

If several of these tethered antennas are launched, each pair of gravity gradient satellites orbiting in east-west direction, then the outputs from each tether array in a cluster can be summed together coherently forming a beam in north-south direction. Coherent addition of inputs and appropriate sequential phasing of outputs can be controlled by computer to generate a scan beam in the horizontal direction (scanned perpendicular to polar axis) resulting in two dimensional scanning.

The above scheme is further refined for application in the publications "Distributed Aperture of Tethered Array Radar Elements" (DATARE) [1], [2].

The gravity gradient tether acts as a one dimensional phased array radar which can scan in a single dimension—in this case the vertical direction. The radiation pattern of a dipole is, $E = \cos(\pi/2 \cos\theta)/\sin\theta$, and hence the intensity of radiation is bidirectional, i.e., E^2 is maximum at $\theta = \pm\pi/2$ (perpendicular to equatorial axis). The directional ambiguity can be resolved by placing a parallel passive tether at $\lambda/4$ separation from the tether con-

0018-9480/92$03.00 © 1992 IEEE

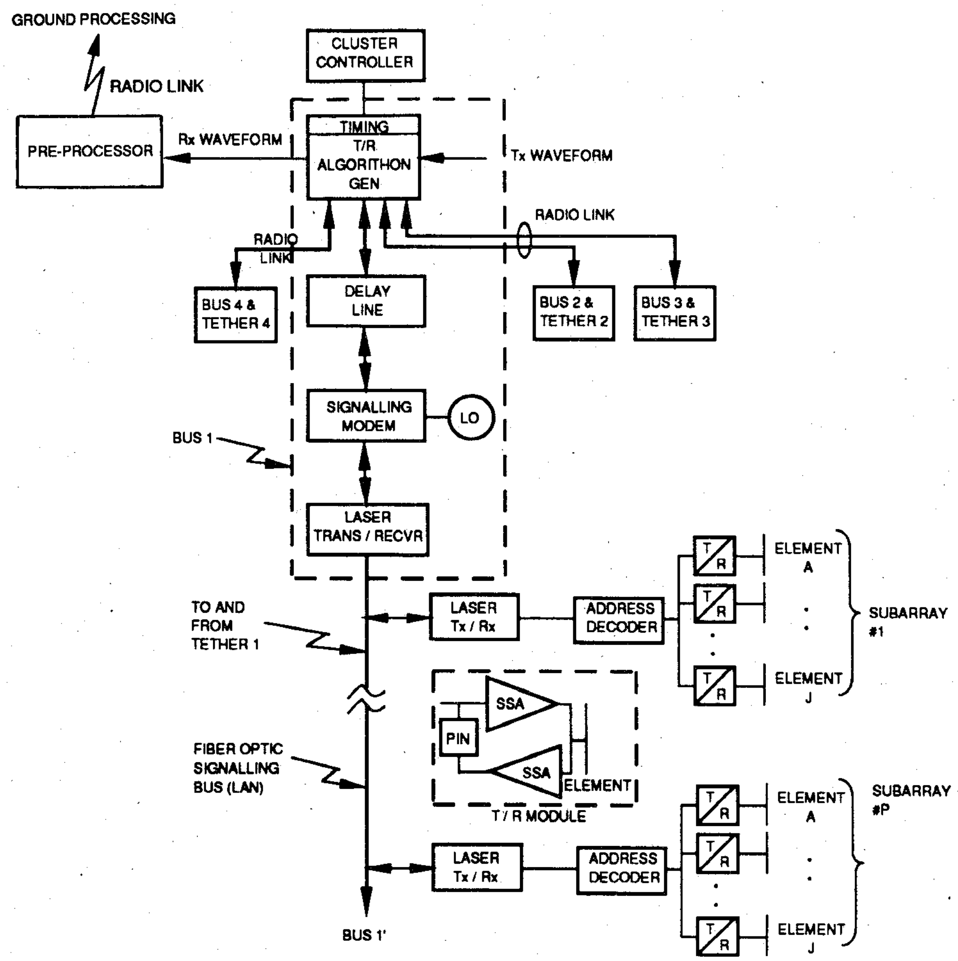

Fig. 2. Overall system architecture.

taining the active elements [2]. Beam formation and scanning issues are discussed later.

II. Trans/Receive Antenna Array [3]

A single-tethered antenna array of dipoles is shown in Fig. 3(a), where an equally spaced linear array of n collinear dipoles is assumed; each element is approximately half wavelength ($\lambda/2$) long and the distance between two successive elements is d where d governs the scan angle and grating lobes for a fixed frequency. Each element has its own Trans/Receive (T/R) module. The T/R waveforms are computer controlled and fed to and from the active elements via a pair of multi-stranded fiber optic cables as shown in Figs. 2 and 3(a). Parallel processing in both satellites is assumed for reliability and rapid processing. The fiber optic cable sheath is assumed to be coated by a thin layer of metallic paint. If this metallic painted cable sheath is placed ($\lambda/4$) apart from the radiating tether, this sheath will act as a reflecting screen thus producing an unidirectional beam eliminating directional ambiguity. The bidirectional radiation pattern of a single dipole is illustrated in Fig. 3(b); the undirection pattern with a reflector is illustrated in Fig. 3(c). The unidirectional n-element pattern is illustrated in Fig. 3(d). Beam scanning in the vertical plane by individual element or a group of elements phase variation is illustrated in Fig. 3(e). Light weight dielectric separators can be provided at appropriate distances to keep the ($\lambda/4$) separation. In addition, these separators can also be used as damping elements to suppress mechanical oscillations of the tether joining two satellites.

A. Radar Frequency

For tether type antenna array the radiating length has been set at a maximum of 6 km and hence at lower frequencies the number of radiating elements is reduced which will require a larger per element transmitting power for a fixed power-aperture product. On the other hand, a higher frequency permits a larger number of radiating elements which require a smaller transmit power per element, however, the tropospheric absorption is also higher at higher frequencies.

From the above considerations it appears the frequency range for SBR will perhaps be limited between 300–1500 MHz. The exact frequency choice must be derived if the system is implemented. However, for further discussion we shall use the upper end of the above range, approximately 1500 MHz.

Since the frequency choice is not specified at this time a maximum tether length of 6 km is chosen. Beyond this

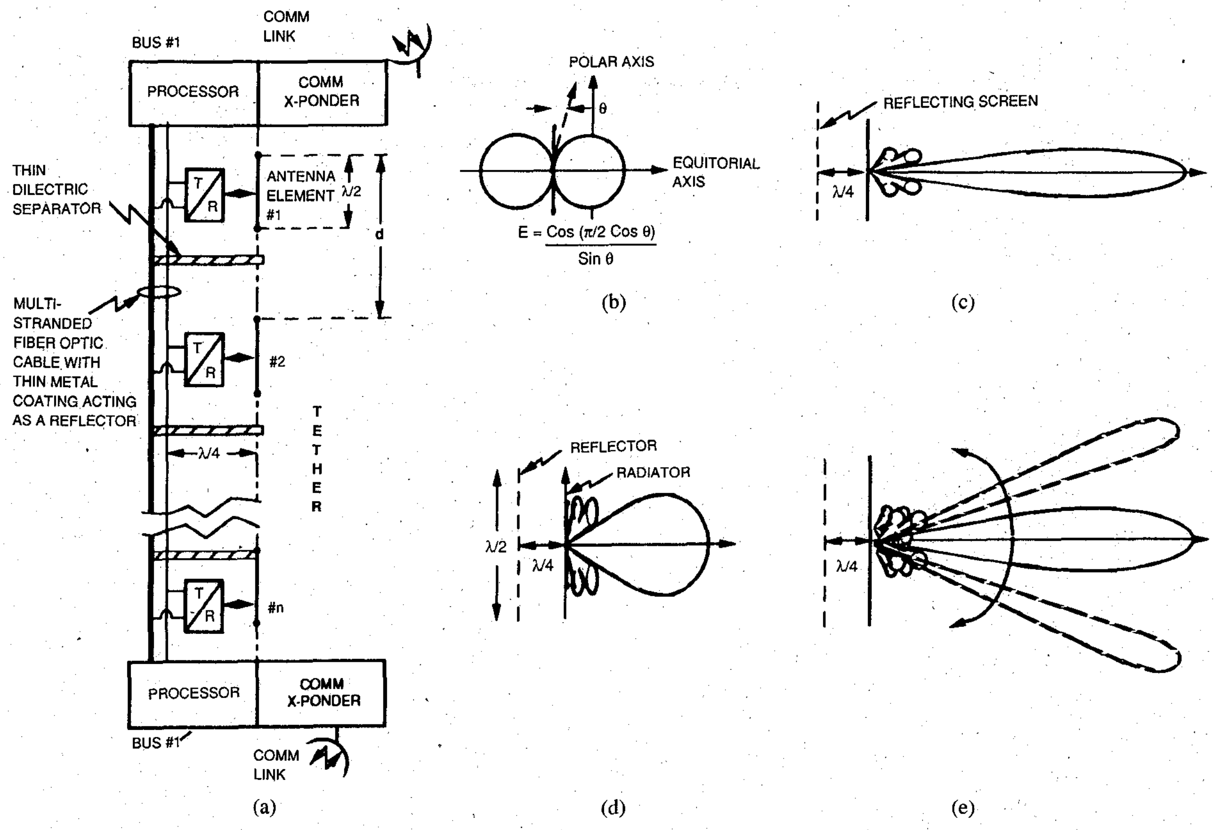

Fig. 3. Trans/received antenna array geometry. (a) Single tethered antenna array configuration. (b) Bidirectional radiation pattern of a single element. (c) Unidirectional pattern with reflector. (d) n-element array pattern. (e) Beam scanning in vertical plane by element phase variation.

length the tether will tend to become unstable. For an actual implementation the length could be shorter depending on the frequency selection.

B. Composite Array Structure by m-Radiating Tethers

The tethered antenna array produces a beam that is narrow in the vertical direction—essentially a thin circular disc as viewed by a distant observer. A moving target within this thin disc, reflecting the transmitted signal will generate Doppler shifts at the receiving apertures which are dependent on the frequency of operation and the relative velocity of the satellite and moving target. If the receiver is designed with a number of matched filters tuned to each probable shift in frequency then the target can be tracked (refer to Fig. 9 for a pulse doppler processing concept). The effects of platform motion can be reduced by electronically displacing the antenna phase center [5].

Using m-tethered antenna arrays, where each vertical tether is parallel to its neighbor but separated by a distance D, m-vertically scanned beams can be produced where each beam is scanned vertically in sequence by varying the phase of each element or a group of elements. If m-array outputs are summed by coherent addition then we have generated a scheme which is equivalent to two-dimensional scanning as illustrated in Fig. 4(a) and (b). Essentially, the system will generate an $m \times n$ - cell scanning scheme where scanning will be generated from on-board processors or by ground controller command.

C. Beam Formation and Coherence

Consider n radiating (or receiving) dipoles in a tether where d is the separation between successive elements as shown in Fig. 5(a) and (b). The output of the summing network can be written as:

$$E(\theta) = \sum_{i=0}^{n-1} a_i \exp\left[j\left(\phi_i + \frac{2i\pi}{\lambda} d \sin\theta\right)\right] \quad (1)$$

where

- $E(\theta)$ is the array factor (same for transmit and receive)
- a_i is the array amplitude taper,
- ϕ_i is the array phase taper,
- θ is the beam direction.

By applying linearly progressive phase increments from element to element or a group of elements by $\Delta\phi$, we can steer the beam direction θ, as follows [3]:

$$\Delta\phi = 2\pi\left(\frac{d}{\lambda}\right)\sin\theta \quad (2)$$

where the (d/λ) parameter also determines the generation of grating lobes within the visible region. The grating lobe will just appear when,

$$\left(\frac{d}{\lambda}\right) = \frac{1}{1+\sin\theta}. \quad (3)$$

To eliminate grating lobes, element spacing should be

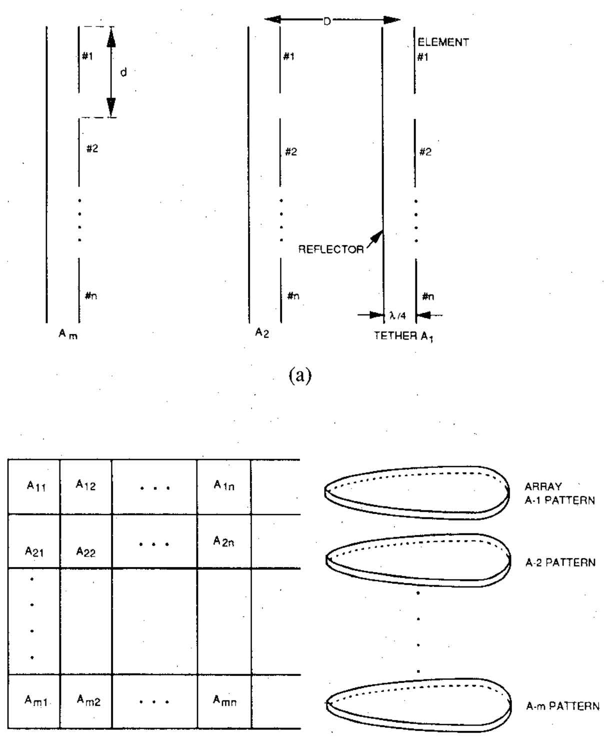

Fig. 4. (a) Composite array with m-parallel tethers. (b) $m \times n$) cells scanning concept.

chosen such that:

$$\left(\frac{d}{\lambda}\right) < \frac{1}{1 + \sin \theta_{\max}}. \tag{4}$$

For example, if the maximum steering angle desired is $\theta_{\max} = \pm 50°$, then $(d/\lambda) < 0.57$. Since this scanning will be performed from a moving platform subjected to perturbations, scan compensation [5] may also be required.

In the composite array of four tethers the nominal separation between two successive tethers is assumed 1.5 km. A separation less than 1.5 km is considered difficult to maintain in gravity gradient low earth orbiting satellites.

Since these tethers are in motion and are subjected to perturbations due to satellite movements the fixed separation will not hold and hence an exact estimation of grating lobes as a function of D (see Fig. 5) is not available at the present time. However, an existing computer simulation [ARRPAT]* has been used at Virginia Tech which indicates that with a constant separation between successive tethers, grating lobes will appear with a fixed delay as illustrated in Fig. 5(a). This delay will allow clamping the grating lobe energy by range gates as shown in Fig. 5(b). A similar argument will hold for sidelobe clutter elimination [5]. An analysis of grating lobe effects and elimination is a subject of further research.

Fig. 5(b) also shows the basic concept of $(m \times n)$ signal component integration by adaptive delay equalization

*W. L. Stutzman and G. A. Thiele, *Antenna Theory and Design*, John Wiley & Sons, Inc. 1981, pp. 572–575.

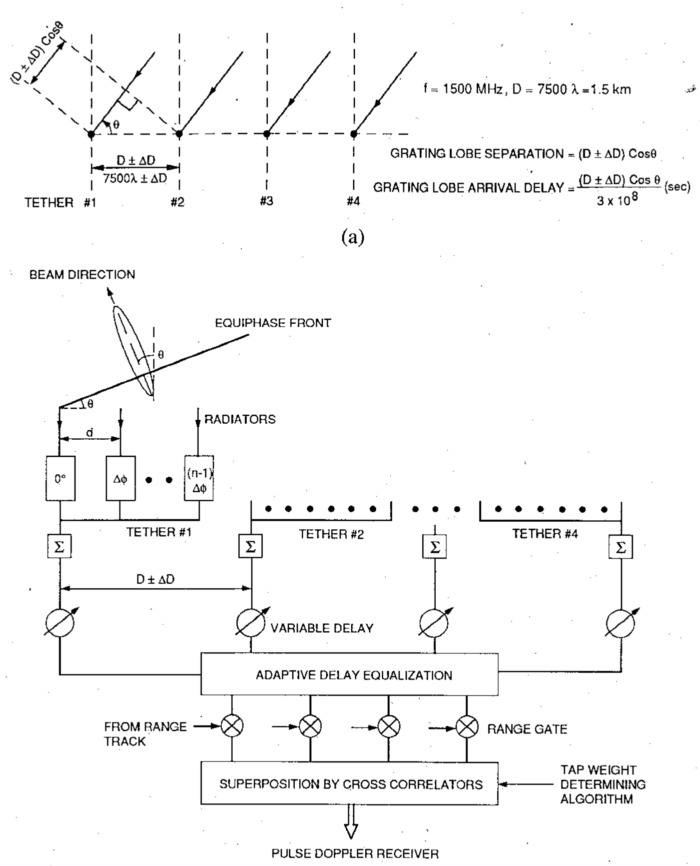

Fig. 5. (a) Grating lobe separation. (b) Basic concept of $(m \times n)$ signal superposition and grating lobe suppression.

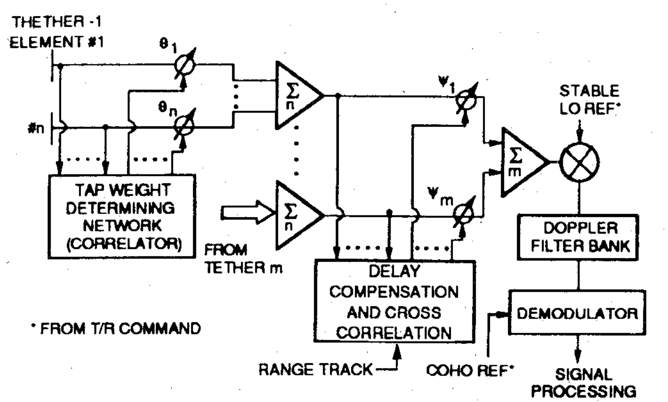

Fig. 6. A simplified schematic of superposition and coherent integration.

(gross compensation) followed by cross correlation (fine compensation). For signal-to-noise ratio maximization the Widrow algorithm [3] is perhaps a better candidate for tap weight determination in cross correlation.

In an ideal case, $(m \times n)$ signal components will superimpose as shown in Fig. 5(b) to maximize the signal-to-noise ratio (S/N), for detection. Thus the overall (S/N) will simply be ρmn where ρ is the (S/N) due to a single dipole. In practice both coherent and noncoherent integration may be necessary.

An implementation concept [4] involving superposition and coherent integration for a pulse Doppler radar is illustrated in Fig. 6, where θ_n represents the phase of the

TABLE I
RANGE CALCULATIONS FOR THREE DIFFERENT TARGET SIZES

σ, Target effective cross section (m^2)/(dB − m^2)	10/10	1.5/1.8	0.25/−6.0
Design Goal S/N, (dB)	20	20	20
$P_t G^2 \lambda^2$ (dBW − m^2)	111.8	111.8	111.8
τ, Lower bound of Integration time (dB − sec)	−10	−10	−10
$(4\pi)^3$ (dB)	33	33	33
kT (dBW)	−200.8	−200.8	−200.8
Range (km)	3090	1930	1230

signal derived by nth element and Ψ_m represents the composite phase of the mth tether signal.

III. RANGE CALCULATIONS

A. Range Equation

$$\frac{S}{N} = \left\{\frac{P_t G^2 \lambda^2 \sigma \tau}{(4\pi)^3 R^4 (kT)}\right\} x \text{ (loss factors)}^{-1} \quad (5)$$

where

P_t = Array cluster average transmit power = mnP = 24 W
mn = number of elements in the cluster = 120 000 (30 000 per tether)
P = Average power per module = 0.2 mW
G = ($m \times n$) matrix antenna gain = 56 dB (element gain with reflector ≃ 5.2 dB)
λ = 0.2 m at 1500 MHz
σ = Target effective reflective area
τ = Integration time = 0.1 − 1 sec
R = Range
k = Boltzman's Constant = 1.38×10^{-23} j/°K
T = Receive System Noise Temp ≃ 600°K (300°K LNA + Hot Earth contribution)
S/N = Signal-to-noise ratio

Integration time will depend on the pulse Doppler signal processing and number of pulses integrated. For the present calculations we have assumed a lower bound of 0.1 sec. The minimum (S/N) required is 17 dB with implementation losses taken into consideration [5]–[7], assuming a non-fluctuating target model with Probability of Detection, $P_D = 0.95$ and False Alarm Probability, $P_{FA} = 10^{-12}$. A system margin of 3 dB is considered desirable. Therefore, a 20 dB (S/N) should be the design goal.

B. Radar Cross Section (RCS) and Range

RCS (σ), study is a very complex subject and its analysis for military targets are classified information. However, an excellent overview of radar cross section of complex objects is available in [8], [9]. Some simulation results of missile RCS estimation are presented in [10]. We now compute range from (5) for 3 different example target sizes namely (Table I),

σ 10 m^2; target at low grazing angle
σ 1.5 m^2; target at intermediate grazing angle
σ 0.25 m^2; target at higher grazing angle

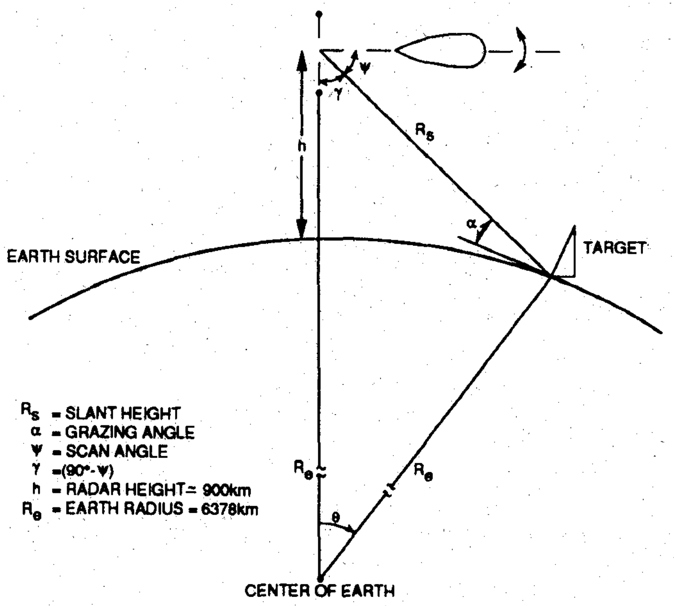

Fig. 7. Slant range geometry.

C. Target Slant Range

The slant range Rs, of the target can be calculated from the geometry as shown in Fig. 7 as follows:

$$Rs = [\mathrm{Re}^2 + (\mathrm{Re} + h)^2 - 2\,\mathrm{Re}\,(\mathrm{Re} + h)\cos\theta]^{1/2} \quad (6)$$

where

$\theta = 90 - (\alpha + \gamma)$
α = Grazing Angle
$\gamma = \sin^{-1}[\mathrm{Re}/(\mathrm{Re} + h)\sin(90 + \alpha)]$
Re = Radius of the earth = 6378 km
$\Psi = 90° - \gamma$ = Scan Angle
h = Radar height (~900 km)

The target slant range Rs, is calculated as a function of α and is shown in Fig. 8 where the range limits for the three RCS's (10 m^2, 1.5 m^2 and 0.25 m^2) are identified. The system under discussion can detect a 10 m^2 target down to about a 4° grazing angle; a 1.5 m^2 target down to approximately 20°; and a 0.25 m^2 target to 43°. In addition to tropospheric absorption, secondary propagation vagaries may become a contributing factor at low grazing angles (4–5 degrees).

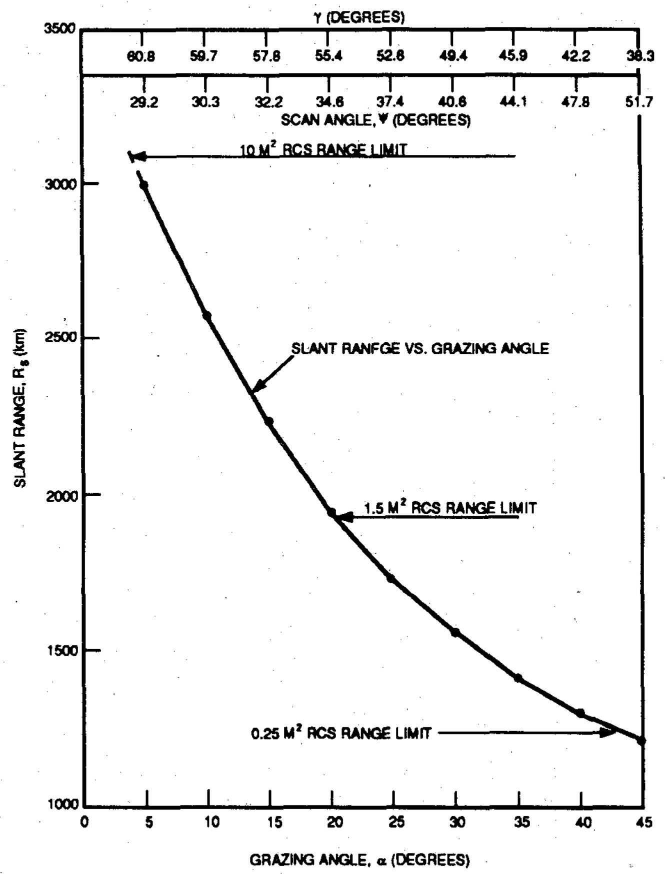

Fig. 8. Slant range versus grazing angle α.

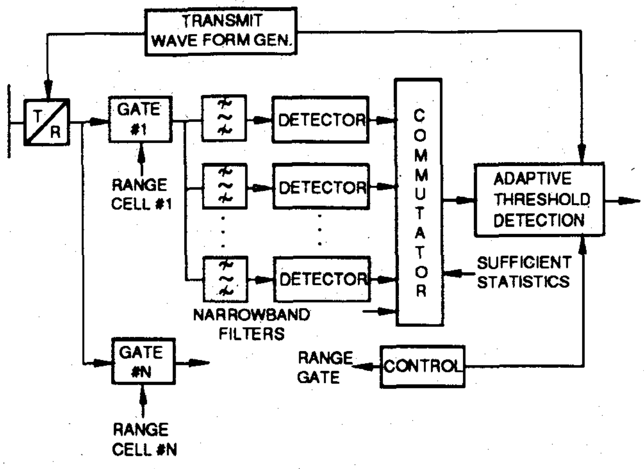

Fig. 9. Pulsed Doppler radar signal processing concept.

IV. Clutter Issues

Clutter is a return signal that is unwanted in the radar situation considered.

In the tethered type of antenna under discussion, the elevation beamwidth is extremely narrow ($\simeq 0.003$ degree). On the other hand, because the source is essentially a line source the azimuthal beamwidth is very wide ($\sim 60°$ with a reflecting screen). As a result, the illuminated sea patch is large which may result in a poor signal-to-clutter ratio [11]. Thus implementation of this scheme is a very challenging task. An in-depth study and simulation with appropriate models will be required to estimate clutter statistics and develop clutter suppression techniques.

The methods of pulse Doppler CFAR (Constant False Alarm Rate) and adaptive threshold processing can perhaps be considered to circumvent the clutter problem. Recently, Lincoln Laboratory developed a technique to achieve clutter rejection [12]. This technique, called a Moving Target Detector (MTD), is an approximation to an optimum clutter rejection filter. A disc memory is used to store stationary clutter returns observed from scan to scan. This allows its removal by the use of adaptive thresholds [13] in range, Doppler, and angle. Also, the MTD technique requires that a number of scan returns be observed (sufficient statistics obtained) before a target is declared present and track on it is initiated. Thus, track initiation is used to help eliminate false clutter returns. Multiple PRF's (or subpulses of different durations) are used to detect weak targets that ordinarily would be masked by clutter. A pulse doppler radar signal processing concept including this type of clutter suppression is outlined in Fig. 9 [11], [12].

V. Communications

We assume each spacecraft will have a processor and a communication transponder on-board. A ground based master control center will have a main frame computer and distributed ground based tracking stations will have some processing capability. For security the master control center function will perhaps be duplicated. A T/R processing concept is illustrated in Fig. 10 where buses (1, 1′), (2, 2′) (3, 3′) and (4, 4′) constitute a cluster of four tethers. Each spacecraft is provided with its own processor, T/R command generator and data handling capability. Bus processors (1, 2, 3, 4) provide the cluster controlling function in a sequential order while bus processors (1′, 2′, 3′, 4′) remain in a standby role and provide increased system reliability. Direct radio communication links between cluster processors exchange T/R command data. Semiprocessed data are sent by Omni-directional broadcast to all other cluster controllers for relaying to ground tracking terminals or to the master control terminal. Each cluster controller also attempts to send its own broadcast data directly to a ground tracking terminal or to the master control center via direct radio links or geosynchronous communications satellites. This scheme essentially makes it a more secure system. Data from cluster controllers and ground tracking terminals can be transmitted via an RA/TDMA (Random Access/Time Division Multiplex Access) channel using a packet switching protocol. The master control center communicates with the cluster controllers via a TDM broadcast channel with multiplexed data packets addressed to different controllers and ground tracking terminals via satellite relay. The communications architecture concept is illustrated in Fig. 11.

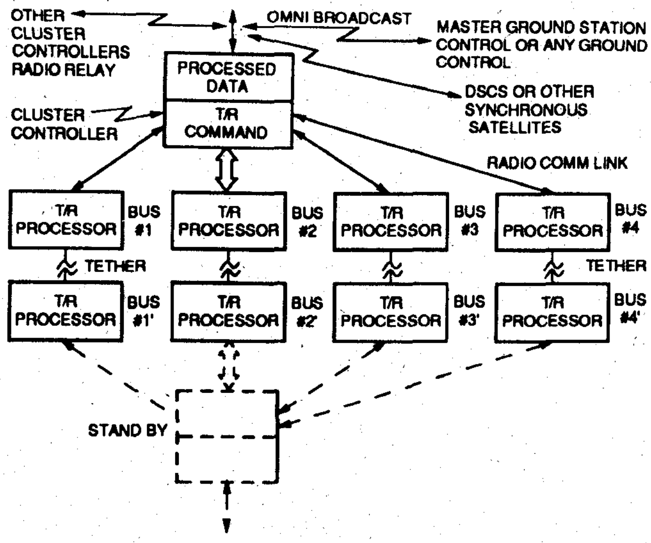

Fig. 10. T/R processing comcept in a cluster.

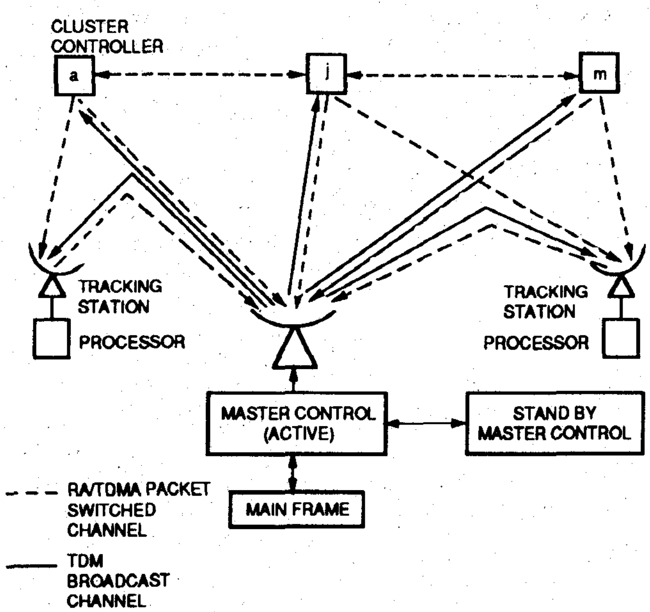

Fig. 11. Communication architecture concept.

VI. System Coverage

The area of the earth *As*, as visible [14] to a cluster of satellites is (Table II)

$$\frac{A_s}{A_t}(\%) = 50(1 - \cos \epsilon) \tag{7}$$

where

A_t = total earth surface area = $4\pi(6378 \text{ km})^2$
ϵ = {arc cos (Re cos α/Re + h) − α}
Re = earth's radius = 6378 km
h = satellite height ≃ 900 km
α = target grazing angle

Cost and complexity will constrain 100% coverage of the earth. Perhaps, 8 to 11 clusters covering nearly one third of the earth is a more practical solution for sea surveillance. Each cluster would consist of four parallel tethers, each tether having 30 000 elements which transmit at 1500 MHz. A total of 64–88 small satellites will therefore be required. Total average transmit power per cluster is 24 W with 0.2 mW/element.

Multi-purpose small satellite development is an ongoing process and it is envisioned that cost-effective small satellites with multiple launch capability per mission will be a fact of life in the early 21st century time frame.

VII. T/R Waveform Signalling and Power Requirements

For T/R signal transmission, a fiber optic LAN is proposed as shown in Fig. 2. A two-level (Mark-Space) noncoherent FSK signalling modem in the LAN with Forward Error Correction (FEC) is suggested. Direct modulation on Distributed Feed Back Laser Diodes (DFB-LD) are suggested as transmitters and InGaAs-PIN Photo Diode receivers may be considered for the laser trans/receiver modules. Low-loss fiber optic cable with loss ~0.2 dB/km and commercial optical couplers with loss ~0.5 dB are available. As an alternative, cost effective LED Trans/Receivers can also be considered. The T/R module can be implemented by a pair of FET amplifiers and a PIN diode switch. A 40-dB on/off ratio can be easily achieved by a single PIN diode.

Power for the T/R modules and laser trans/receivers can either be generated by distributed solar cells along the tether elements or it can be provided from a power bus by paralleling the prime power sources of the two satellites supporting the tether (storage batteries will complement power requirements when the sun is not visible). The later scheme is in essence what is used in under-sea fiber optic links.

VIII. Tether Stability

It has been demonstrated [1] that tethers are stable platforms for radio communications. However, long tethers exhibit some minor fluctuation effects. In addition to a small residual libration, the tether will be subjected to some perturbations due to,

Finite satellite relative movements
(East-West and North-South)
Air drag
Lunar and solar gravity
Radiation pressure.

Typical examples of tether bowing and libration simulation results are shown in Figs. 12 and 13, respectively. The finite bowing and libration as shown above will have negligibly affects in tether stability but must be considered when analyzing coherent operation. However, these small perturbations can also be controlled as discussed below.

Libration can be controlled by varying the tether length (difficult to implement in an operation system).

TABLE II
SYSTEM REQUIREMENTS SUMMARY

Grazing Angle (degree)	5	10	15	20
Visible Earth Surface (%)	4.4	3.1	2.2	1.6
Total no. of clusters required for 100% coverage	23	32	45	63
Total no. of satellites per cluster (2 per tether)	8	8	8	8
No. of satellites reqd. for continuous 100% coverage	184	256	360	504
No. of satellites reqd. for 50% coverage	96	128	184	256
No. of satellites reqd. for 33% coverage	64	88	120	168

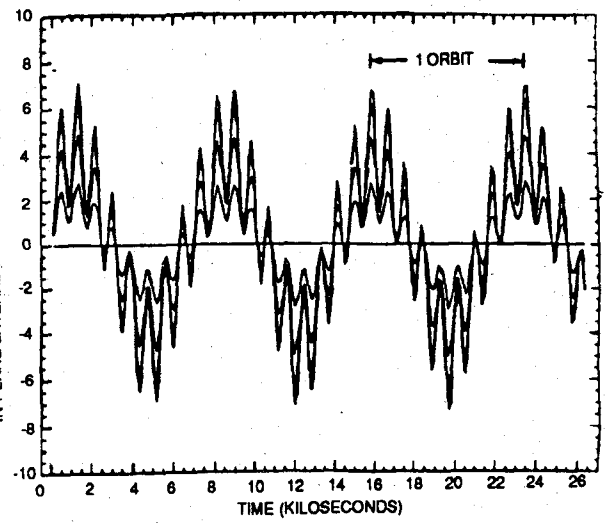

Fig. 12. Tether bowing.

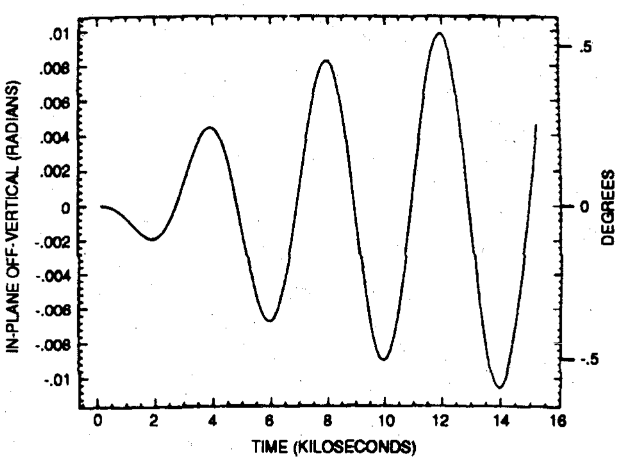

Fig. 13. Tether libration.

Tether bowing can be damped by mechanical dampers (see Fig. 3), such as light dielectric separators across the tether length.

Finite east-west and north-south movement of the satellites will produce a gyroscopic movement which can be damped by either eddy current dampers or magnetic torques on board the satellite buses.

IX. CONCLUSION

A space-based microwave radar concept for sea borne target detection is defined using multipole dipole trans/receive elements streched between two small gravity gradient, low earth orbiting satellites. A cluster of radars is comprised of four 6 km long tethers each separated from the next tether nominally by 1.5 km. Each tether is comprised of 30 000 T/R elements which operate at 1500 MHz. Power consumption per cluster is about 24-W resulting a slant range of about 3000 km for a target size of 10 m^2 at about 5° grazing angle.

Clutter suppression is the most challenging task involved for practical implementation of this scheme. Coherence of multiple tether outputs also deserves careful consideration.

ACKNOWLEDGMENT

The late Dr. Harry Davis' contribution to this Space-based radar concept is gratefully acknowledged. Acknowledgement is also made to Prof. W. Stutzman for some useful discussions. Finally, thanks are due to the editor and four reviewers for their critical reviewing and editing of the manuscript.

This paper is mainly based upon a feasibility study undertaken by the author of Fairchild Space Company which was subsequently submitted to Rome Air Development Center as an alternate space based radar scheme resulting in a definition study contract with Decision Science Applications as the prime contractor and Fairchild Space Company as one of the subcontractors. Revisions of the original manuscript have been carried out at JPL.

REFERENCES

[1] *Tether in Space Handbook*, Prepared for NASA, Aug. 1986.

[2] P. G. Tomlinson, T. C. Brown, and D. Chakraborty, "Space-Based Tethered Array Radar (STAR) - A Distributed Small Satellite Network," in *Proc. 14th DARPA Strategic System Symp.*, University of Utah, Oct. 24–27, 1988.

[3] R. C. Johnson and H. Jasik, *Antenna Engineering Handbook*, 2nd ed. New York: McGraw Hill, 1984.

[4] A. S. Acampora, "High Power Radar Implementation of Coherent Waveforms," *IEEE Trans. Aerosp. Electron. Syst.*, July 1976.

[5] M. I. Skolnik, *Radar Handbook*. New York: McGraw Hill, 1990.

[6] D. K. Barton, *Radar System Analysis*. Englewood Cliffs, NJ: Prentice-Hall, 1964.

[7] R. S. Berkowitz, *Modern Radar*. New York: Wiley, 1961.
[8] *Proc. IEEE*, May 1989, Special Issue on Radar Cross Section of Complex Objects.
[9] R. E. Kell, "On the derivation of bistatic RCS from monostatic measurements," *Proc. IEEE*, pp. 983-988, Aug. 1965.
[10] J. I. Glaser, "Some results in the bistatic radar cross section (RCS) of complex objects," *Proc. IEEE*, May 1989.
[11] J. L. Eaves and E. K. Reedy, *Principles of Modern Radar*. New York: Van Nostrand Reinhold, 1987.
[12] E. Brookner, *Radar Technology*. Norwood, MA: Artech House, 11th Printing, 1986.
[13] D. Chakraborty, K. Kato, and R. Lei, "Consideration of 120-Mbits/s burst mode adaptive threshold detection with estimated sequence processor development," in *Proc. Sixth Int. Conf. on Digital Satellite Communications*, Phoenix, AZ, Sept. 19-23, 1983.
[14] R. L. Freeman, *Reference Manual for Telecommunications Engineers*. New York: Wiley, 1985.

D. Chakraborty (M'68-SM'77) received the Ph.D. degree in microwave physics from the University of Surrey, England in 1967.

He is currently associated with California Institute of Technology, Jet Propulsion Laboratory. He was with Fairchild Industries from February 1985 to February 1990 and prior to that he was with COMSAT Laboratories for 16 years where he made significant contributions in high-speed digital satellite communications engineering. During 1961-1968, he was employed by the British Post Office Research Department, Dollis Hill, London, where he was engaged in satellite communications and microwave engineering. During 1959-1961, he was employed by Decca Radar, Radar Development Laboratory, Chessington, Surrey, England.

Dr. Chakraborty is a Fellow of the IEE, London. He served as the chairman of IEEE National Capital Area Continuing Education Committee. He also served as the chairman of the IEEE AES Washington-N. Va. Chapter.